Shear Flow Effect on the Crystalline Forms in Polyamide 6/Montmorillonite Nanocomposites

Ivan Kelnar, Jaroslav Kratochvíl, Jana Mikešová

Institute of Macromolecular Chemistry AS CR, 162 06 Prague 6, Czech Republic

Received 16 March 2007; accepted 21 June 2007
DOI 10.1002/app.27021
Published online 21 August 2007 in Wiley InterScience (www.interscience.wiley.com).

ABSTRACT: The influence of shear flow on the crystallization of polyamide 6/MMT nanocomposites prepared by melt intercalation process was investigated in detail by differential scanning calorimetry. The melted nanocomposites were controlled sheared in the steady and oscillatory shear flow, using a rotational rheometer, and cooled in an inert atmosphere. The effects of shear rate or frequency, clay concentration, and crystallization conditions on PA 6 crystalline phase development were studied. As expected, an opposite impact of shearing on γ-phase formation in the nanocomposites and neat matrix was found. Surprisingly, a critical shear frequency for the onset of γ-form crystallinity formation in the nanocomposites, increasing with the filler content as a consequence of polymer chains confinement within oriented clay platelets was found. At higher shear frequencies, the proportion of γ-form in the nanocomposites increased dramatically with the clay concentration and reached 30–40%. The shear flow effects were influenced by cooling conditions, and more significant effect for rapidly cooled samples was observed. The isothermal crystallization at the solidification temperature 205°C reduced the γ-form content. © 2007 Wiley Periodicals, Inc. J Appl Polym Sci 106: 3387–3393, 2007

Key words: polymer nanocomposites; PA6, γ-form crystallinity; flow-induced crystallinity; DSC

INTRODUCTION

Considering changes in polymer crystalline structure by a filler addition, a complex knowledge of clay effects on the matrix crystallization is also required for successful nanocomposite investigations.

Crystallinity of the exfoliated polyamide 6/montmorillonite (PA6/MMT) nanocomposite, i.e., a system containing delaminated platelets, homogenously dispersed in the matrix, is significantly influenced by the clay and is a subject of numerous studies.[1–14] Because of space restrictions between clay platelets, both the crystallization kinetics and crystalline morphology of the matrix are changed. The significant feature of PA6/MMT nanocomposites is the formation of an increased portion of γ crystallinity, a polymorphic form consisting of parallel-aligned hydrogen-bonded chains, (lower packing density, monoclinic, or pseudohexagonal). The γ-form occurs in neat PA 6, usually, only after rapid melt cooling[15] and is unstable, transforming to the stable monoclinic α-form consisting of fully extended planar zigzag chains, in which adjacent antiparallel chains are joined to each other by hydrogen bonds during storage.

Correspondence to: I. Kelnar (kelnar@imc.cas.cz).
Contract grant sponsor: Grant Agency of the Czech Republic; contract grant number: 106/03/0679.

In PA6 nanocomposites, the clay surface induces kinetically favored formation of γ-phase, occurring predominantly near clay platelets.[16] In contrast to the neat PA 6, the γ-form crystallinity is stable,[17,18] as a result of the polymer chains confinement of MMT[1,19] and is also the main reason for properties improvement.[20] An increase in the γ-phase content by annealing at 80°C was reported for extruded nanocomposites.[21] The mentioned polymer chain confinement together with the γ-nucleating effect of the clay may also lead to a modification of the γ-phase as reported, e.g., by Nair and Ramesch[22] A further characteristic feature of the nanocomposites is the substantial orientation level in PA6 crystalline regions,[23,24] observed even at high mold temperature (90°C) in injection molding.[25–27] Owing to specific interactions of PA chains with MMT, the crystallinity is influenced by polymer chain orientation near the clay surface;[28,29] the epitaxial growth of crystallinity starts from a chain tethered to the clay surface. The crystalline structure of PA 6/clay composites is also influenced by processing and thermal treatment.[30–32]

An important factor influencing generally crystallization of polymers through oriented or stretched chains and, consequently, their material properties is the shear applied during processing.[33–35] The effects of shear on crystallization temperatures or even on supercooled melt in polyolefins were studied. The importance of this phenomenon for PA 6 is documented by numerous works dealing with drawing

of fibers.[36–40] It is evident that in PA6 nanocomposites more significant shear effects on the matrix crystallization should be expected considering a preferential orientation of exfoliated platelets through shear flow. Weon et al.[41] recently studied the effect of large-scale shear in extrusion at 60°C on the orientation of PA 6 crystalline lamellae and confirmed the important role of the platelets orientation in the process. Study[42] of the time-resolved shear behavior of end-tethered PA6/clay nanocomposites by through-view SAXS patterns showed that the nanocomposites can be oriented under relatively low shear rates (60 s^{-1}) and at temperatures immediately above the melting temperature. The authors conclude that the exfoliated clay is the primary reason for inducing the oriented γ-form under shear, because the nanocomposites crystallize in this form also without shear.

It was found that no detailed study of shear flow effect on the γ-phase formation in the presence of MMT has appeared. The present work, focused on this aspect, was motivated by our recent finding that, in PA6/MMT nanocomposite, prepared by melt compounding, annealing for 15 min at 270°C and cooling slowly, only α-phase was detected. No γ-phase was also found in the nanocomposites solidified in a thin layer at 160 and 205°C. The mentioned findings were observed on thin layer samples, thermally treated in ''steady'' state on the hot stage of a polarizing microscope and in DSC apparatus with the same regime. Similar to our observation, preferential crystallization of the α-form was also found for slowly cooled *in situ* polymerized PA 6/MMT sample.[43] On the other hand, our attempt to prepare a nanocomposite containing dominant α crystallinity under similar solidification and annealing conditions of injection molding was not successful. To analyze our observation, we indicated an important role of flow in the γ-phase formation in PA 6/MMT nanocomposites.

The goal of the present work is to assess the role of shear flow in the crystallization of molten polyamide nanocomposites. For this purpose, the crystallinity of the nanocomposites subjected to various shearing conditions in the molten state before solidification was observed.

EXPERIMENTAL

Materials

The organoclay used in the study was commercial product Cloisite 30B (Southern Clay Products, Gonzáles, TX), a natural montmorillonite (MMT) modified by alkylbis(2-hydroxyethyl)methylammonium chloride with the alkyl derived from hydrogenated tallow (clay content 74 wt %). The cation exchange capacity of the clay is 90 mequiv 100 g^{-1} and interlayer spacing 1.85 nm.

Polyamide 6 (PA6) was the commercial grade (Ultramid B5, BASF, Germany) with M_n = 42,000.

Nanocomposites preparation

Prior to mixing, PA6 and clay were dried at 85 and 70°C, respectively, for 12 h in a vacuum oven. The nanocomposites were prepared by mixing the components in the W 50 EH chamber of a Brabender Plasti-Corder at 255°C and 45 rpm for 10 min. The material was immediately compression-molded at 250°C to form 1-mm-thick plates. Strips cut from these plates were used for the preparation of disc samples in a laboratory microinjection molding machine (DSM Research, Netherlands). The barrel temperature was 265°C, and that of mold 80°C. When molded, the samples were used for shear flow experiments. The clay contents were 1, 3, and 5 wt % of Cloisite 30B (not corrected for the neat silicate content). Structure and properties of the nanocomposites showed well dispersed and high-exfoliated organoclay in the matrix; their structure and material characteristics were published in our previous papers.[44,45]

Shear-treated nanocomposites preparation

a. Controlled shear flow

Using an ARES 3 rotational rheometer (Rheometric Scientific, Piscataway, NJ) with the parallel-plate geometry of 25-mm diameter and the 1 mm gap between the plates, nanocomposites with flow-induced crystallization were prepared. The nanocomposites were melted at 270°C for 3 min between the plates before the gap setting and kept 10 min at rest before shearing. Because of problems with melt ejection from the rheometer gap during steady shear flow, oscillatory shear flow experiments were preferred for shearing because no flow disturbances occurred in the used frequency range. Comparing DSC thermograms of selected nanocomposites deformed with both types of flow, the identical influence of shearing on γ-form crystallization was observed for the same values of shear rate and shear frequency. The oscillatory shear flow experiments were carried out for 5 min at the 7% strain and at a constant frequency between 0 and 100 rad s^{-1}.

b. Nanocomposites crystallization

The melts of nanocomposites were cooled down in two different ways after shearing:

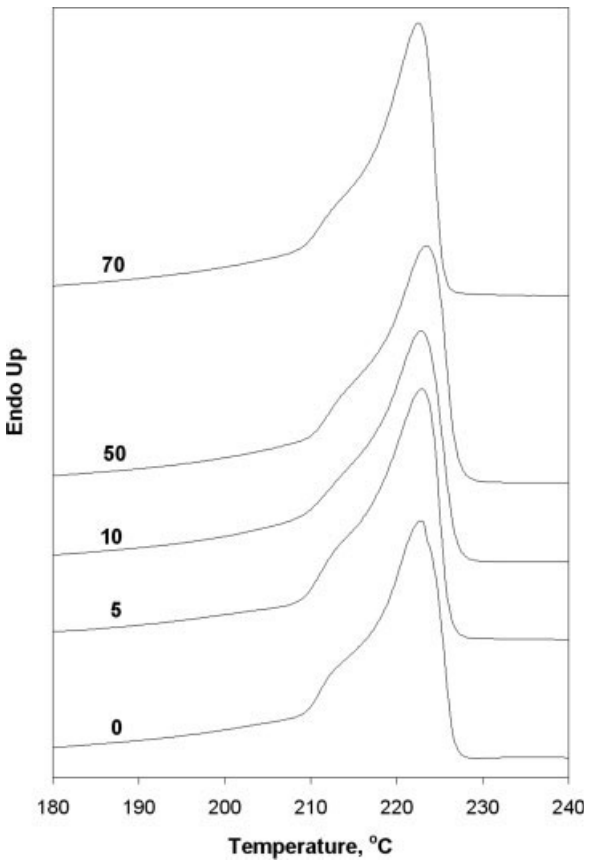

Figure 1 Melting endotherms of annealed nanocomposites PA6 + 3% MMT after flow at respective shear frequencies (rad s^{-1}).

1. Nonisothermal crystallization—rapid cooling (R samples)—a small piece of the melt was scraped out from the gap of a rheometer and rapidly cooled to laboratory temperature immediately after shearing;
2. Isothermal crystallization + Annealing (A samples)—the melt was cooled for 2 min to the solidification temperature 205°C and annealed for 30 min in the gap of rheometer.

The shearing of melts and subsequent isothermal crystallization with annealing in rheometer were performed under nitrogen to prevent degradation of the matrix.

Differential scanning calorimetry

A Perkin-Elmer Pyris 1 DSC apparatus was employed for calorimetric measurements. The samples of about 10 mg were sealed in aluminium pans, and the system was cooled with liquid nitrogen and flushed with helium. Indium and cyclohexane were used for calibrating the temperature and heat-flow scales. The DSC runs were scanned in the temperature interval from 80 to 260°C at a heating rate 10°C min^{-1}. The samples were measured immediately after shear treatment as two series—annealed and rapidly cooled, as described earlier. For verification of stability of the γ-form, three selected samples were also measured after 1-month storage at laboratory temperature.

RESULTS AND DISCUSSION

The results of DSC measurements are summarized in Figures 1 through 7. The thermograms show the main melting endotherm of the crystalline α-form of the polyamide at about 223°C. The endotherm of the γ-form, if present, appears at about 212°C; in some samples it appears just as a hump on the ascending branch of the α-form endotherm or is missing at all. At 190–200°C, some rapidly cooled samples show a flat exotherm, indicating probably additional crystallization of polyamide after releasing the segmental motion in amorphous parts on heating.

The DSC scans of the nanocomposites of PA6 containing 3% MMT crystallized isothermally at 205°C after flow at respective shear frequencies (ω) are shown in Figure 1. The thermograms are quite

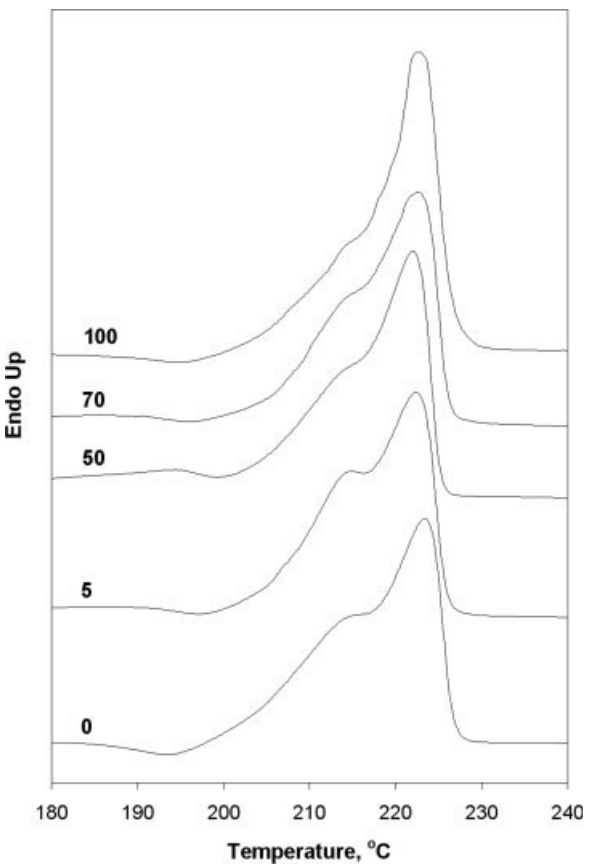

Figure 2 Melting endotherms of nonisothermally crystallized neat PA6 after flow at respective shear frequencies (rad s^{-1}).

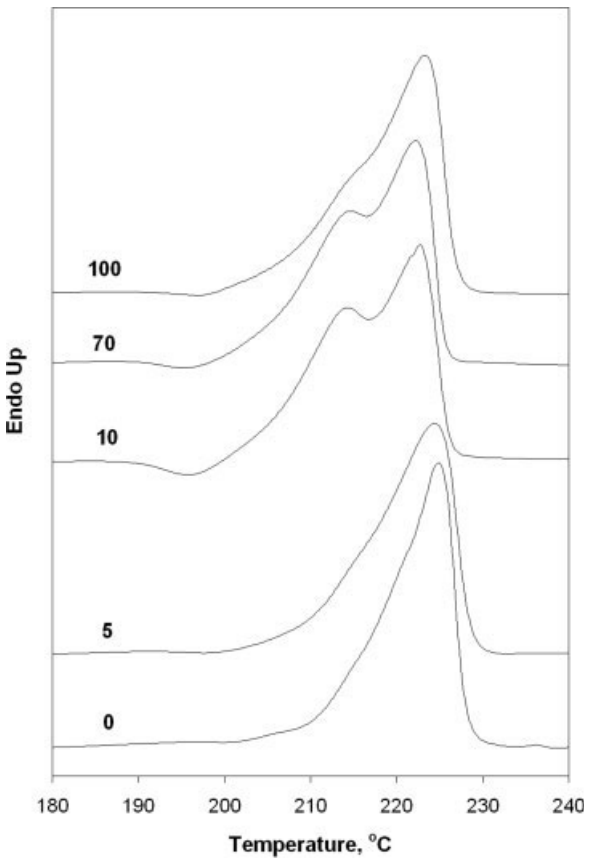

Figure 3 Melting endotherms of nonisothermally crystallized nanocomposites of PA6 + 1% MMT after flow at respective shear frequencies (rad s^{-1}).

similar and show the main endotherm of the α-form at about 223°C with just small proportions of the γ-form, which does not change with frequency. The thermograms do not include any exotherm at 190–200°C, which means that crystallization was completed during annealing at 205°C and subsequent cooling to laboratory temperature. The heat of fusion of the annealed samples of PA6 + 3% MMT does not change with ω. Its average value is 65.7 J g^{-1} corresponding to PA6 crystallinity of about 29%. Comparing the value with the crystallinity of a sample with analogous thermal history prepared by injection molding of the melt into a mold heated to 205°C and 30-min storage in the mold, the higher content γ-form in the latter case is most probably a consequence of more intensive shear flow during injection molding. We again recommend that without any flow, only α-crystallinity was present for the same thermal history. These results indicate the important effect of shear flow on the γ-crystallinity formation. This effect is clearly seen from more ''*in situ*'' observations of the melt rapidly cooled immediately after shearing, indicating the undisturbed effect of flow on the γ-crystallinity evolution (and its influence by different concentrations of clay).

Figure 2 shows the DSC thermograms of neat PA6 rapidly cooled after treatment at various shear frequencies. The proportion of the γ-form expressed as the hump at about 212°C is significant at zero and low frequencies, decreasing with increasing frequency. All thermograms show the flat exotherm at about 195°C associated with additional crystallization of undercooled polyamide chains on heating. The crystallinity of flow-treated PA6 samples did not show any significant change with shear frequency. Its average value was 24.6%, a value considerably smaller than the usually stated 50–60% for crystallinity of equilibrated neat PA6. Untreated PA6 used in this study had crystallinity of about 48%.

In the case of nanocomposites containing 1 and 3% of organoclay (Figs. 3 and 4), significant amounts of the γ-form were found at intermediate shear frequencies. These samples showed similar crystallinities (24.5% on average) as those of neat shear-treated PA6.

Figure 5 shows that the dependence of the γ-form content on the shear frequency for the rapidly cooled PA6 nanocomposite containing 5% organoclay has a character opposite to that of neat polyamide (Fig. 2). At zero frequency, the sample of nanocomposite

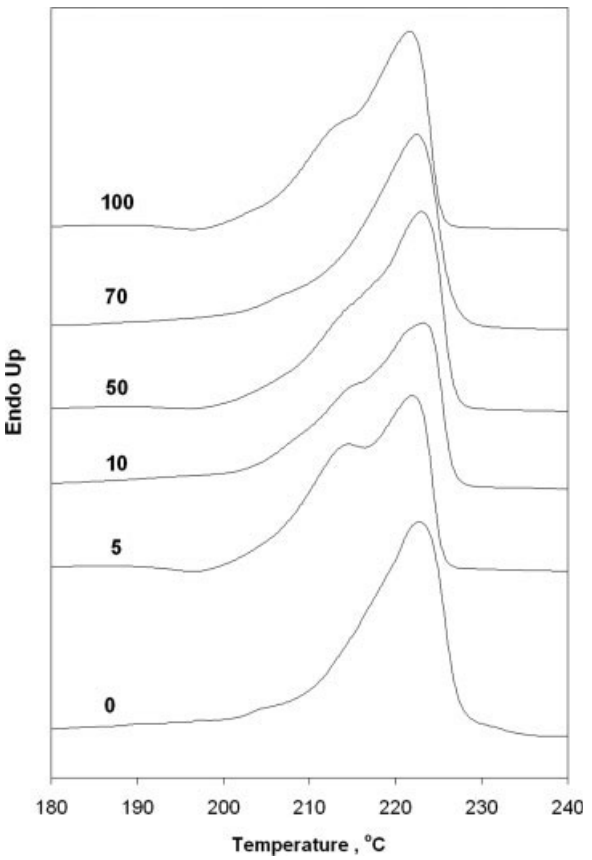

Figure 4 Melting endotherms of nonisothermally crystallized nanocomposites of PA6 + 3% MMT after flow at respective shear frequencies (rad s^{-1}).

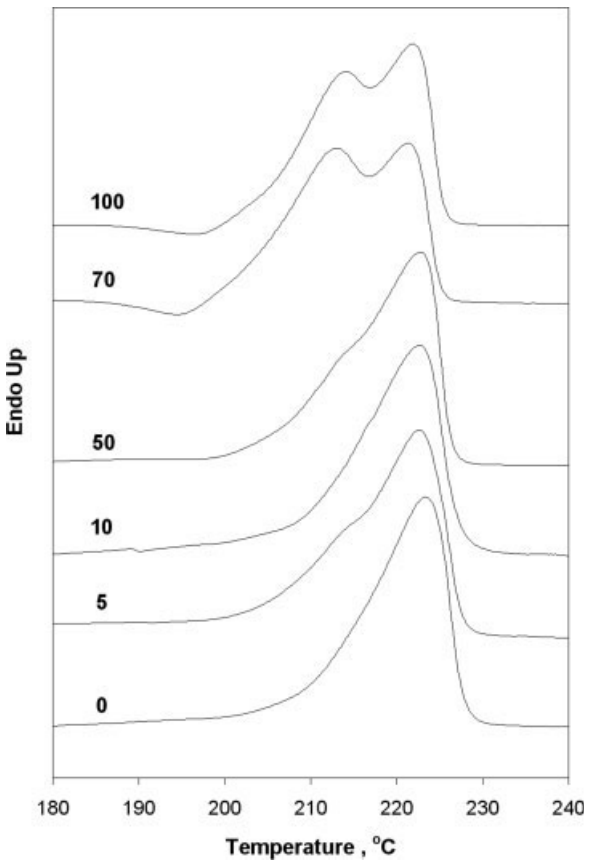

Figure 5 Melting endotherms of nonisothermally crystallized nanocomposites of PA6 + 5% MMT after flow at respective shear frequencies (rad s^{-1}).

contains no γ-form, whereas at high frequencies (70 and 100 rad s^{-1}) the proportion of the γ-form is quite significant—estimated at some 30–40%. Average crystallinity of nanocomposite PA6 + 5% MMT was 23.6%, somewhat lower than for neat PA6 and lower-MMT nanocomposites, and showed a slightly decreasing dependence on shear frequency. Unlike for all the earlier described results (Figs. 1–4), where no change with frequency was found for the peak temperature of the α-form endotherm, a decreasing trend between 223.3 and 221.4°C for frequency rising from 0 to 100 rad s^{-1} was detected for nanocomposite PA6 + 5% MMT. This result suggests a trend that the higher the clay content the higher the shear flow necessary for the γ-form evolution. This finding corresponds with literature data indicating, e.g., geometric restriction caused by clay. Probably cooperative local ordering of clay and PA6 chains caused by flow promotes extended chain crystallization.

Figure 6 summarizes results of the study of the organoclay content effect on crystallization behavior of the nanocomposites at two extreme frequencies (0 and 100 rad s^{-1}). At the frequency $\omega = 0$ rad s^{-1}, the proportion of the γ-form decreases with the clay content. Average crystallinity was 24.7% with no dependence on clay concentration. At the frequency $\omega = 100$ rad s^{-1}, on the contrary, the proportion of the γ-form in neat polyamide is very low, increasing dramatically with the clay content, reaching ~30–40% for 5% MMT. Crystallinity decreases from 25.2% for neat PA6 to 22.9% for nanocomposite PA6 + 5% MMT.

In order to detect stability of the γ-form in the studied shear-treated nanocomposites, three samples were also measured after 1-month storage at laboratory temperature, viz. annealed PA6 + 3% MMT and rapidly cooled PA6 + 3% and 5% MMT (see Fig. 7). In all three tested samples, the γ-form disappeared during the 1-month storage at laboratory temperature. The stored, rapidly cooled samples also did not show any exotherm of additional crystallization. No change in overall crystallinity (about 28%) and peak temperature of the α-form (223.0°C) was detected in the annealed sample. On the contrary, crystallinity increased from 24 to 28% and from 23 to 26.5%, and the peak temperature of the α-form from 222.0°C to 224.4°C and from 221.4°C to 223.7°C for the rapidly cooled samples of PA6 + 3% and 5% MMT, respectively. This indicates that the 1-month

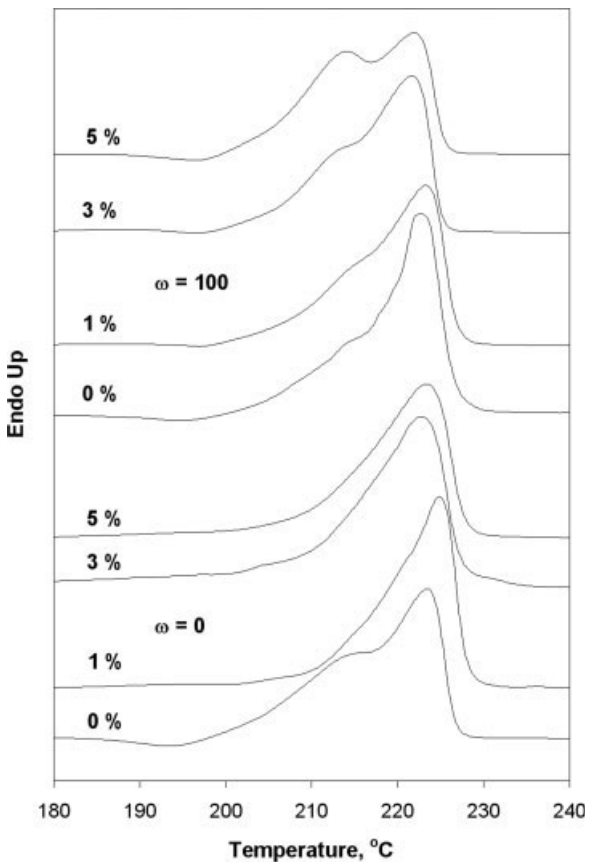

Figure 6 Melting endotherms of nonisothermally crystallized nanocomposites of PA6, containing respective concentrations of MMT after flow at shear frequencies $\omega = 0$ and 100 rad s^{-1}.

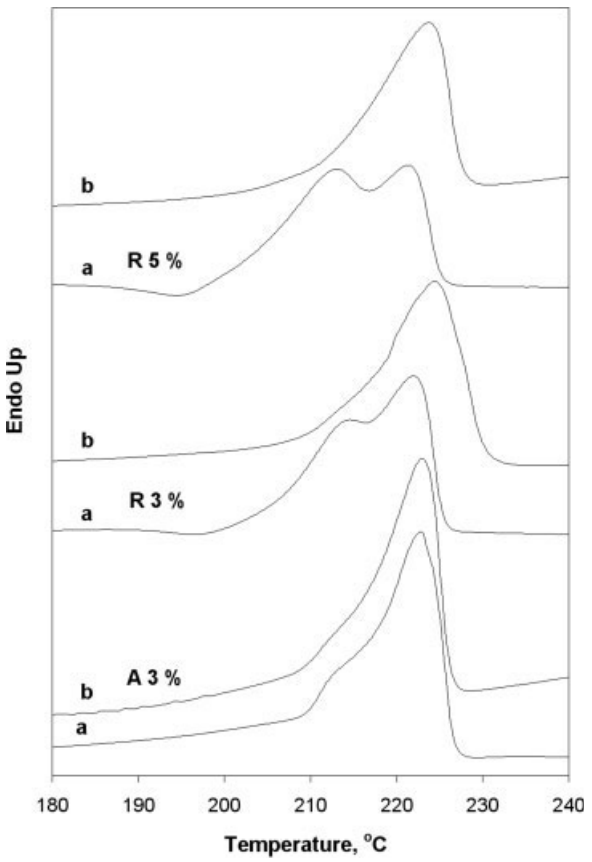

Figure 7 Melting endotherms of nanocomposites of PA6: annealed (A) + 3% MMT, rapidly cooled (R) + 3% and 5% MMT measured: (a) after shear flow, (b) after 1-month storage under dry conditions at laboratory temperature.

storage at laboratory temperature of the rapidly cooled shear-treated PA6 nanocomposites is associated not only with disappearance of the crystalline γ-form but also with an increase in total crystallinity to the value comparable with that of the annealed samples, and with overall perfection of the α-form crystallites. The last results are in contrast to crystallinity of injection-molded samples (with more intensive shearing before solidification, which is usually done at temperatures about 80°C), where a significant content of γ-crystalline phase exists after much longer storage and even thermal treatment. Probably, the applied shear leads to less-developed (and stable) γ-crystalline phase; this is indicated by different melting temperature and stability. Unfortunately, the restrictions of rheometer construction did not allow a study on more wide velocity range, but even the results obtained describe well the importance of shear for γ crystallinity in the clay-restricted system.

CONCLUSIONS

The present results indicate a dominant effect of flow on the γ crystalline phase formation in melt-mixed, highly exfoliated PA6/MMT nanocomposite. Within the studied flow conditions (small deformation oscillatory shear, frequency 0–100 rad s^{-1}) performed at 270°C, with lower clay contents, even a critical interval of shear frequency was found, at which only the γ crystalline form appeared. This critical shear frequency increased (higher shearing was necessary for the onset of γ crystalline phase formation) with elevated clay content as a consequence of geometric restrictions imparted by clay.

References

1. Lincoln, D. M.; Vaia, R. A.; Wang, Z. G.; Hsiao, B. S.; Krishnamoorti, R. Polymer 2001, 42, 9975.
2. Mathias, L. J.; Davis, R. D.; Jarrett, W. L. Macromolecules 1999, 32, 7958.
3. Kojima, Y.; Matsuoka, T.; Takahashi, H.; Kurauchi, T. J Appl Polym Sci 1994, 51, 683.
4. Wu, Q.; Liu, X.; Berglund, L. A. Macromol Rapid Commun 2001, 22, 1438.
5. Liu, X.; Wu, Q.; Berglund, L. A.; Qi, Z. Macromol Mater Eng 2002, 287, 515.
6. Liu, X.; Wu, Q. Eur Polym J 2002, 38, 1383.
7. Lincoln, D. M.; Vaia, R. A.; Krishnamoorti, R. Macromolecules 2004, 37, 4554.
8. Mathias, L. J.; Davis, R. D.; Jarrett, W. L. Macromolecules 1999, 32, 7958.
9. Bureau, M. N.; Denault, J.; Cole, K. C.; Enright, G. D. Polym Eng Sci 2002, 42, 1897.
10. Privalko, V. P.; Karaman, V. M.; Privalko, E. G.; Lehmann, B.; Friedrich, K. J Macromol Sci B 2003, 42, 975.
11. Dinzhos, R. V.; Privalko, E.G.; Privalko, V. J Macromol Sci B 2005, 44, 421.
12. Liu, X.; Wu, Q. Eur Polym J 2002, 38, 1383.
13. Liu, X.; Wu, Q.; Berglund, L. A. Macromol Mater Eng 2002, 287, 515.
14. Liu, X.; Breen, Ch. Macromol Rapid Commun 2005, 26, 1081.
15. Puffr, R.; Kubánek, V., Eds. Lactam-Based Polyamides, Vol. I; CRC Press: Boca Raton, 2000.
16. Wu, Q.; Liu, X.; Berglund, L. A. Polymer 2002, 43, 2445.
17. Akkapedi, M. K.; Polym Compos 2000, 21, 576.
18. Wu, T. M.; Chen, E. Ch.; Liao, Ch. S. Polym Eng Sci 2002, 42, 1141.
19. Tol, R. T.; Mathot, V. B. F.; Reynaers, H.; Goderis, B.; Groeninckx, G. Polymer 2005, 46, 2966.
20. Usuki, A.; Koiwai, A.; Kojima, Y.; Kawasumi, M.; Okada, A.; Kurauchi, T.; Kamigaito O. J Appl Polym Sci 1995, 55, 119.
21. Xie, S.; Zhang, S.; Liu, H.; Chen, G.; Feng, M.; Quin, H.; Wang, F.; Yiang, M. Polymer 2005, 46, 5417.
22. Nair, S. S.; Ramesch, C. Macromolecules 2005, 38, 454.
23. Kojima, Y.; Usuki, A.; Kawasumi, M.; Okada, A.; Kurauchi, T.; Kamigaito, O.; Kaji, K. J Polym Sci Part B: Polym Phys 1994, 32, 625.
24. Kojima, Y.; Usuki, A.; Kawasumi, M.; Okada, A.; Kurauchi, T.; Kamigaito, O.; Kaji, K. J Polym Sci Part B: Polym Phys 1995, 33, 1039.
25. Kojima, Y.; Usuki, A.; Kawasumi, M.; Okada, A.; Kurauchi, T.; Kamigaito, O.; et al. J Polym Sci Part B: Polym Phys 1995, 33, 1039.
26. Yalcin, B.; Cakmak, M. Polymer 2004, 45, 2691.
27. Yalcin, B.; Valladares, D.; Cakmak, M. Polymer 2004, 44, 6913.
28. Devaux, E.; Bourbigot, S.; Achari, A. E. J Appl Polym Sci 2002, 86, 2416.

29. Kawasumi, M. J Polym Sci Part A: Polym Chem 2004, 42, 819.
30. Liu, X. H.; Wu, Q. J.; Zhang, Q. X.; Berglund, L. A.; Mo, Z. S. Polym Bull 2002, 48, 381.
31. Fornes, T. D.; Paul, D. R. Polymer 2003, 44, 3945.
32. Illers, K. H.; Haberkorn, H.; Simak, P. Makromol Chem 1972, 158, 285.
33. Zhang, Ch.; Hu, H.; Wang, D.; Yan, S.; Han, Ch. C. Polymer 2005, 46, 8157.
34. Kumaraswami, G.; Issaian, A. M.; Cornfield, J. A. Macromolecules 1999, 32, 7537.
35. Abuzaiana, F. M.; Fitz, B. D.; Andjelič, S.; Jamiolkovski, D. D. Polymer 2002, 43, 4699.
36. Murthy, N. S.; Aharoni, S. M.; Szollosi, A. B. J Polym Sci Polym Phys Ed 1985, 23, 2549.
37. Stepaniak, R. F.; Garton, A.; Carlsson, D. J.; Wiles, D. M. J Polym Sci Polym Phys Ed 1979, 17, 987.
38. Murthy, N. S. Polym Commun 1991, 32, 301.
39. Miyasaka, K.; Ishikawa, K. J Polym Sci A-2: Polym Phys 1968, 6, 1317.
40. Hiramatsu, N.; Hirakawa, S. Polym J 1982, 14, 165.
41. Weon, J. I.; Xia, Z. Y.; Sue, H. J.; J Polym Sci Part B: Polym Phys 2005, 43, 3555.
42. Medellin-Rodriguez, F. J.; Burger, C.; Hsiao, B. S.; Chu, B.; Vaia, R.; Phillips, S. Polymer 2001, 42, 9015.
43. Puffr, R. unpublished results.
44. Kelnar, I.; Kotek, J.; Munteanu, B. S.; Kaprálková, L. J Appl Polym Sci 2006, 96, 288.
45. Kelnar, I.; Kotek, J.; Kaprálková, L.; Hromádková, J.; Kratochvíl, J. J Appl Polym Sci 2006, 100, 1571.